

MODELLING OF THE CONJUGATE NATURAL CONVECTION IN A CLOSED SYSTEM WITH THE RADIANT HEATING SOURCE RADIANT ENERGY DISTRIBUTION BY LAMBERT'S COSINE LAW

by

Geniy V. KUZNETSOV and Alexander E. NEE*

National Research Tomsk Polytechnic University, Tomsk, Russia

Original scientific paper

<https://doi.org/10.2298/TSCI160120256K>

Various types of emitters are often used as energy sources in real engineering systems and technological processes. Investigations of heat transfer basic laws in such systems are of interest. We conducted mathematical modelling of conjugate heat transfer in a closed rectangular cavity under conditions of radiant energy source operating. The 2-D problem of conjugate natural convection in vorticity-stream function-temperature dimensionless variables has been numerically solved by means of the finite difference method. Radiant energy distribution along the gas-wall interfaces was set by Lambert's cosine law. We obtained fields of temperature and stream functions in a wide range of governing parameters (Rayleigh number $10^4 \leq Ra \leq 10^6$, the length of radiant heating source $0.15 \leq D \leq 0.6$). Then we analyzed how heat retaining properties of finite thickness heat conducting walls made of different materials affect the heat transfer intensity. Differential characteristics distribution showed significant non-uniformity and non-stationarity of the conjugate heat transfer process under study.

Key words: *infrared emitter, natural convection, conjugate heat transfer, mathematical modelling, Lambert's cosine law*

Introduction

Infrared radiation, as one of the relatively safest types of radiant energy, is actively engaged in agroindustry [1-3], at composite [4], polymeric [5] and wood [6] materials drying. In addition, infrared emitters can be applied for heating of locally located working zones in large scale premises [7]. However, use of gas infrared emitters is limited due to the lack of theoretical studies on applications of radiant heating systems. Based on the results of the study [7], a reasonable conclusion can be made that natural convection plays an important role in formation of temperature fields in the cavities heated by gas infrared emitters. For this reason the basic laws of heat transfer are reasonable to investigate in order to increase the energy efficiency of such power supply systems.

Studies of convective energy transfer regimes play an important role in science and engineering. Solutions of various natural convection problems in closed and semi-open cavities in non-conjugate [8-14] and conjugate [15-18] formulation are published. However, a special interest for practical applications represents investigation of jointly proceeding processes of conduction, convection, and radiation.

* Corresponding author, e-mail: nee_alexander@mail.ru

Hamimid and Guellal [19] conducted mathematical modelling of laminar natural convection under conditions of the surface thermal radiation in a square cavity filled by air with internal source of energy. The 2-D heat transfer problem was solved by means of the finite volume method. The authors [19] paid particular attention to the impact of the emissivity and internal energy source on the formation of isotherm and streamline contours in the solution domain. It was established that an increase in the value of internal energy source led to a significant modification of the temperature and streamline fields. Moreover, variation of this parameter led to the secondary convective cell formation. This factor increased the temperature in the entire solution domain.

Kolsi *et al.* [20] analyzed the effect of the radiative heat transfer and aspect ratio on regimes of the 3-D natural convection at fixed Prandtl ($Pr = 13.6$) and Rayleigh ($Ra = 10^5$) numbers. The complex heat transfer equations were formulated in terms of the vorticity – stream function – temperature variables and solved by means of the finite volume method. It was established that variation of the conductive-radiative parameter led to a significant modification of the temperature and stream function fields. Quasi-2-D flow was formed near the median plane in the absence of radiation. The impact of the radiation heat transfer on the 3-D regimes of fluid-flow was significant in the center of the cavity.

Montiel-Gonzalez *et al.* [21] conducted numerical simulation of laminar natural convection under conditions of the thermal surface radiation in a square cavity with vertical open boundary. The equations of continuity, momentum, and energy in the primitive variables were solved by means of the finite volume method and the SIMPLEC algorithm. Problem formulation assumed that thermophysical properties of air were temperature-dependent. Theoretical analysis was conducted in the Rayleigh number range of $10^4 \leq Ra \leq 10^6$. Dimensionless temperature difference, φ , between the hot wall and the bulk fluid varied from 0.333-1.333. According to the numerical simulation results, it was established that the total Nusselt number increased by 79.8% ($Ra = 10^6$) and 88.0% ($Ra = 10^4$) when φ was varied from 0.333-1.333. Moreover, radiation was pre-dominant heat transfer mechanism for large dimensionless temperature differences ($0.667 \leq \varphi \leq 1.333$), which was proved by the values of heat fluxes and average Nusselt numbers.

Nouanegue *et al.* [22] conducted mathematical modelling of conduction, natural convection, and radiation in an inclined square cavity bounded by solid thermally conductive wall on one side. Left vertical wall was with the stationary heat flux. Right vertical wall assumed isothermal. The 2-D equations of mass, momentum, and energy conservation under Boussinesq approximation were solved by means of the finite difference method and SIMPLER algorithm. Various parameters were Rayleigh number ($10^8 \leq Ra \leq 3 \cdot 10^{10}$), dimensionless conductivity of bounding wall ($10 \leq k_r \leq 40$), dimensionless wall width ($0 \leq w \leq 0.15$), inclination angle ($60 \leq \varphi \leq 150$) the surface emissivity ($0 \leq \varepsilon \leq 1$). It was established that convective heat flux was significantly decreasing function of the surface thermal radiation. The impact of the thermal conductivity and width of the solid wall on the average Nusselt number at the bottom horizontal boundary was insignificant. Radiative Nusselt number was independent from the variation of the inclination angle. It should be noted that the solid thermally conductive wall did not affect to the heat transfer modes, which was obviously due to the solution of the steady heat conduction equation.

Saravanan and Sivaraj [23] conducted theoretical analysis of impact of surface thermal radiation on natural convection modes in the air-filled cavity with the heated thin plate. Vertical walls and plate assumed isothermal. Radiant flux was supplied to the horizontal boundaries. Equations of mass, momentum, and energy transfer were solved by means of the finite volume method on a uniformly staggered grid. The impact of governing parameters, viz., Rayleigh number

($10^5 \leq Ra \leq 10^7$), dimensionless plate length ($0.25 \leq D \leq 0.75$) and orientation (horizontal and vertical) on the non-conjugate heat transfer modes were studied in detail. It was established that radiative heat transfer led to non-uniform distribution of isotherms in the cavity. Moreover, temperature gradient between horizontal walls was decreased. Heat transfer rate was higher when the plate was oriented vertically.

An approach [24] based on numerical solution of Navier-Stokes equations in the modify vorticity-stream function variables was suggested for thermal regime analysis of domains with the radiant heating sources when solving heat transfer problems in conjugate formulation. Investigations of fundamental laws of conduction and convection processes were carried out for the semirestricted [24] and closed [25, 26] domains under conditions of the thermogravitational heat exchange. Numerical analysis [26] was performed for four possible cases of radiant energy distribution along the gas-solid wall interfaces in laminar flow regime. But the problem statement [24-26] assumed that the emitter thickness was infinitely small in comparison with the characteristic sizes of the solution domain. This assumption significantly simplifies the numerical realization of the natural convection process under study. But, at the same time, a question about the impact estimation of geometrical characteristics of the infrared emitter (its surface temperature can achieve 500 K) on the thermal regime of the heated system is left open. Therefore, the heat transfer analysis under operating conditions of radiant energy source is of interest.

In addition, the real thermal state of the heating source and possibility of heat transfer due to the gas conduction near the emitter were not taken into account [24-26]. This factor in a certain range of parameters can significantly affect to the heat transfer rate.

The aim of this study is the numerical investigation of the heated system under conditions of radiant energy distribution along rectangular cavity interfaces and analysis of the effect of the infrared emitter's geometrical characteristics on the thermal regime.

Problem formulation and solution method

Geometrical and physical models

We considered the unsteady process of the conjugate heat transfer by natural convection. The solution domain is presented as a rectangular cross-section cavity filled with gas and limited by thermally conductive walls of finite thickness. We assumed that the surface temperature of the radiant heating source was time-independent. Equalities of temperatures and heat fluxes were set at the gas-wall interfaces. The conditions of thermal insulation were assumed at the external boundaries of the solution domain. The gas was considered as an absolutely transparent medium for heat radiation. We conducted a numerical investigation in the laminar flow regime. The radiant energy distribution along the interfaces of the rectangular cavity was defined by Lambert's cosine law [11]. In accordance with this law, the radiant intensity observed from an ideal diffusely reflecting surface or ideal diffuse radiator is directly proportional to the cosine of the angle γ , fig. 1, between the direction of the incident light and the surface

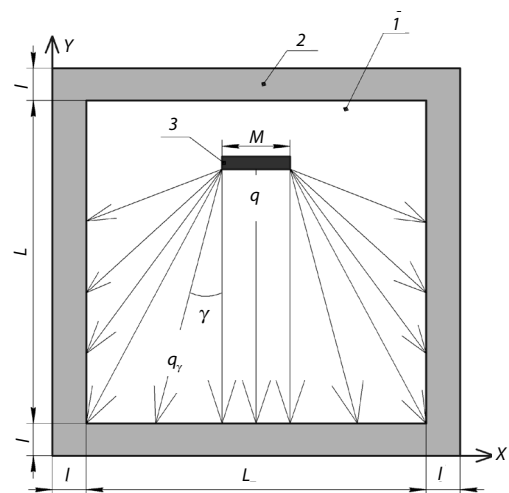


Figure 1. Solution domain; 1 – thermally conductive walls, 2 – air, 3 – radiant energy source

normal ($q_r = q \cos \gamma$). We assumed that reflector was set at the top horizontal boundary of the radiant heating source. Therefore, radiant flux was supplied only to the bottom horizontal and vertical gas-wall interfaces.

The problem formulation assumed that the gas was viscous incompressible fluid under Boussinesq approximation. Thermophysical properties of the air and enclosures were considered as temperature-independent.

Mathematical model

The conjugate natural convection under study is described by a system of the unsteady 2-D equations of Boussinesq-Oberbek (in modified variables) and energy for the gas and the heat conduction equations for the enclosures and radiant energy source. The boundary value problem was formulated in terms of vorticity-stream function-temperature dimensionless variables. We used a transverse size of the gas cavity as the scale of the distance. To reduce the system of equations to the dimensionless form we used the following relationships:

$$X = \frac{x}{L}, \quad Y = \frac{y}{L}, \quad \tau = \frac{t}{t_0}, \quad U = \frac{u}{V_{nc}}, \quad V = \frac{v}{V_{nc}}$$

$$\Theta = \frac{T - T_0}{T_h - T_0}, \quad \Psi = \frac{\psi}{\psi_0}, \quad \Omega = \frac{\omega}{\omega_0}, \quad V_{nc} = \sqrt{g\beta(T_h - T_0)L}, \quad \psi_0 = V_{nc}L, \quad \omega_0 = \frac{V_{nc}}{L}$$

The dimensionless equations of vorticity transport, Poisson, and energy for the gas in the natural convection regime and the heat conduction equations for the enclosures and radiant energy source are [12, 13, 27]:

$$\frac{\partial \Omega}{\partial \tau} + \frac{\partial \Psi}{\partial Y} \frac{\partial \Omega}{\partial X} - \frac{\partial \Psi}{\partial X} \frac{\partial \Omega}{\partial Y} = \sqrt{\frac{\text{Pr}}{\text{Ra}}} \left(\frac{\partial^2 \Omega}{\partial X^2} + \frac{\partial^2 \Omega}{\partial Y^2} \right) + \frac{\partial \Theta_1}{\partial X} \quad (1)$$

$$\frac{\partial^2 \Psi}{\partial X^2} + \frac{\partial^2 \Psi}{\partial Y^2} = -\Omega \quad (2)$$

$$\frac{\partial \Theta_1}{\partial \tau} + \frac{\partial \Psi}{\partial Y} \frac{\partial \Theta_1}{\partial X} - \frac{\partial \Psi}{\partial X} \frac{\partial \Theta_1}{\partial Y} = \frac{1}{\sqrt{\text{RaPr}}} \left(\frac{\partial^2 \Theta_1}{\partial X^2} + \frac{\partial^2 \Theta_1}{\partial Y^2} \right) \quad (3)$$

$$\frac{\partial \Theta_2}{\partial \tau} = \text{Fo}_2 \left(\frac{\partial^2 \Theta_2}{\partial X^2} + \frac{\partial^2 \Theta_2}{\partial Y^2} \right) \quad (4)$$

$$\frac{\partial \Theta_3}{\partial \tau} = \text{Fo}_3 \left(\frac{\partial^2 \Theta_3}{\partial X^2} + \frac{\partial^2 \Theta_3}{\partial Y^2} \right) \quad (5)$$

The initial conditions for the eqs. (1)-(5) are:

$$\Psi(X, Y, 0) = 0, \quad \Omega(X, Y, 0) = 0 \quad (6)$$

$$\Theta_1(X, Y, 0) = \Theta_2(X, Y, 0) = \Theta_3(X, Y, 0) = 0 \quad (7)$$

The boundary conditions for the eqs. (1)-(5) are:

– at the surface of the radiant heat source:

$$\Theta = 1 \quad (8)$$

– at the external boundaries of the solution domain:

$$\frac{\partial \Theta}{\partial n} = 0 \quad (9)$$

– at the gas-solid wall interfaces parallel to X axis:

$$\Psi = 0, \quad \frac{\partial \Psi}{\partial Y} = 0, \quad \begin{cases} \Theta_i = \Theta_j, \\ \frac{\partial \Theta_i}{\partial Y} = \frac{\lambda_j}{\lambda_i} \frac{\partial \Theta_i}{\partial Y} + \text{Ki}, \end{cases} \quad \text{where } \begin{cases} i = \overline{1,2} \\ j = \overline{1,2} \end{cases} \quad (10)$$

– at the gas-solid wall interfaces parallel to Y axis:

$$\Psi = 0, \quad \frac{\partial \Psi}{\partial X} = 0, \quad \begin{cases} \Theta_i = \Theta_j, \\ \frac{\partial \Theta_i}{\partial X} = \frac{\lambda_j}{\lambda_i} \frac{\partial \Theta_i}{\partial X} + \text{Ki}, \end{cases} \quad \text{where } \begin{cases} i = \overline{1,2} \\ j = \overline{1,2} \end{cases} \quad (11)$$

Numerical procedure

Differential eqs. (1)-(5) with the corresponding initial (6), (7) and boundary (8)-(11) conditions were solved by means of the finite difference method on a uniform grid (151×151). Equations (1)-(5) were solved consecutively. Each time step began with calculating of the temperature field in the wall – gas – wall system. Then we solved Poisson eq. (2) and calculated boundary conditions for vorticity transport eq. (1) according to the Woods formula [28]. Next eq. (1) was solved.

We used the locally 1-D scheme of Samarskiy [29] to approximate eqs. (1)-(5). In this scheme, solution of 2-D equations is reduced to the consecutive solution of 1-D equations. Convective terms were approximated by applying the difference scheme of the second order. Diffusion terms were approximated by applying the central differences. In order to make this scheme independent from the sign of velocity, we conducted approximation smoothing of the convective terms U and $|U|$ (V and $|V|$), respectively. The 1-D difference analogues, which were obtained after discretization, were solved by the sweep method [28]. Approximation of the boundary conditions had the second order of accuracy. In order to select the grid size, we performed grid-dependence test. The results of this test are presented in fig. 2.

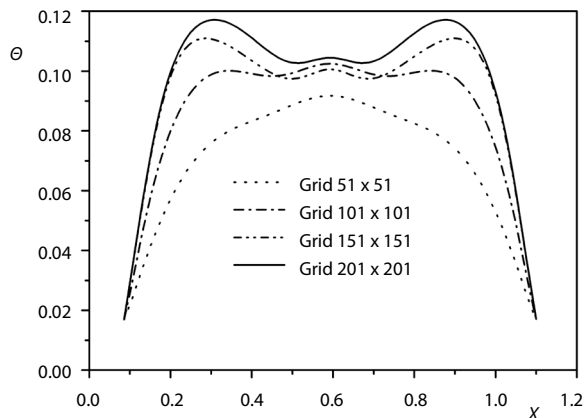


Figure 2. Temperature distributions in the gas cavity in the cross-section of $Y = 0.6$

Validation

We have tested the solution algorithm used on a model problem of natural convection [30] in a closed square cavity with adiabatic horizontal and isothermal vertical walls. The average Nusselt number was used as a characteristic of the heat transfer process and calculated:

$$\text{Nu}_{\text{av}} = \int_0^1 \left| \frac{\partial \Theta}{\partial X} \right|_{X=0} dY$$

The test results are presented in tab. 1.

Table 1. Comparison of the average Nusselt numbers

Ra	Nu _{av} [30]	Nu _{av} [31]	Nu _{av} [32]	Nu _{av} [10]	This study		
					Mesh 64 x 64	Mesh 256 x 256	Mesh 512 x 512
10 ³	1.118	1.121	1.108	1.113	1.119	1.096	1.01
10 ⁴	2.243	2.286	2.201	2.254	2.28	2.213	2.11
10 ⁵	4.519	4.5463	4.43	4.507	4.7315	4.515	4.651
10 ⁶	8.799	8.652	8.754	8.802	9.562	8.897	8.742

With reference to the analysis of the presented average Nusselt number values, tab. 1, we have made a reasonable conclusion that this algorithm can be successfully applied for the solution of such problems.

Results and discussion

Numerical investigations of conduction and natural convection under conditions of the radiant energy distribution according to the Lambert's cosine law were conducted for the following values of parameters: $10^4 \leq Ra \leq 10^6$, $0 \leq Ki \leq 7$, $0.1 \leq D \leq 0.75$, $0^\circ \leq \gamma \leq 90^\circ$, $Pr = 0.71$. The results of numerical simulation are presented in terms of the temperature and stream function fields. The main attention was given to the unsteady factor, analysis of the heat-retaining properties of thermally conductive finite thickness walls and impact of the Rayleigh number on the temperature fields and streamlines formation.

Investigation of the non-stationarity factor

Figure 3 presents the isotherms in the gas cavity for various length of the radiant heating source.

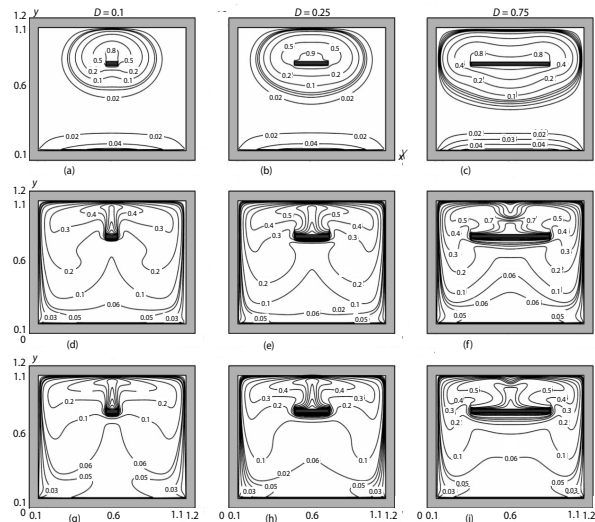


Figure 3. Isotherms for various transverse sizes of the radiant heating source and $Ra = 10^6$; (a), (b), (c) $\tau = 10$, (d), (e), (f) $\tau = 100$, (g), (h), (i) $\tau = 300$

From the analysis of the temperature fields, fig. 3, it could be concluded that the heat transfer process under study was time-dependent. The area of high temperature was formed near the radiant heating source with $\tau = 10$. The radiant flux, which came from the infrared emitter to the gas-wall interfaces, initiated a rise in the temperature of these boundaries. An increase in the length of the radiant heating source resulted in a significant increment of the average temperature in the gas cavity under otherwise equal conditions. Natural convection effects were slight at this value of dimensionless time, $\tau = 10$. With increase of time to 100 temperature fields, figs. 3(d)-3(f), were modified significantly. When $D = 0.75$, fig. 3(f), the ascending air-flow near the radiant heating source was decelerated by the descending counter moving flow in the cross-section of $Y = 0.9$. A convective torch was formed at the upper horizontal surface of the

emitter. A further increase in dimensionless time, $\tau = 300$, led to a rise in the temperature in the area between the radiant heating source and the upper horizontal wall of the solution domain. When $D = 0.75$, fig. 3(i), the vertical size of the convective torch increased, which was obviously due to the moving of isotherm $\Theta = 7$ to the top horizontal wall. The impact of the non-stationarity factor was clearly observed on the temperature distributions in the characteristic sections, figs. 4(a), and 4(b).

Figure 4 presents temperature distributions in the cross-section of $X = 0.6$ in the gas cavity, which illustrate significant unsteadiness of the conjugate heat transfer process under study. An increase in the dimensionless time led to a rise in the temperature at the bottom horizontal gas-wall interface, which was due to intensive supply of energy to this interface. Air heating in the area of $0.5 < Y < 0.66$, fig. 4(a), near the radiant heating source occurred by conduction. An increase in the temperature in the area of $0.8 < Y < 1.07$, fig. 3(b), was due to the formation of the convective torch at the top horizontal surface of the infrared emitter.

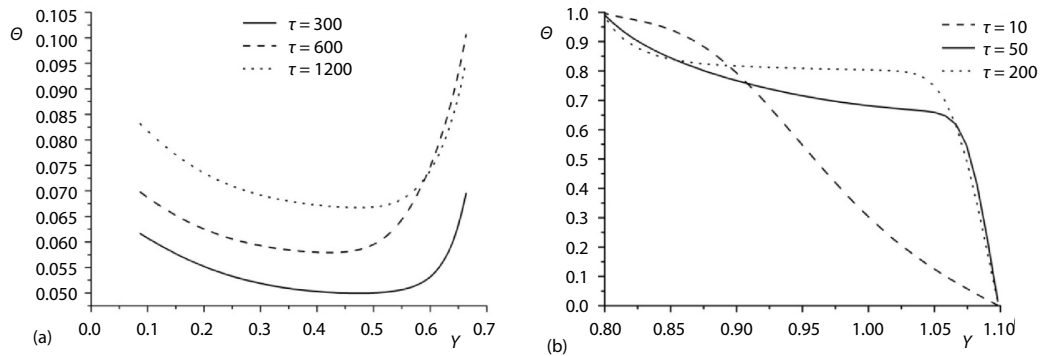


Figure 4. Temperature distributions with $Ra = 10^6$ and $D = 0.25$ in the cross-section of $X = 0.6$

Figure 5 shows the stream function fields illustrating the flow pattern. The hot air ascended along the Y -axis as a result of the natural convection. When the upper horizontal interface of the solution domain was reached, the air was cooled due to the heat losses to the walls. Then the gas descended along the vertical boundaries. When $\tau = 10$, figs. 5(a)-5(c), two symmetrical large-scale convective cells were formed in the gas cavity. At this value of dimensionless time, the infrared emitter length did not affect to the flow pattern. An increase in the time to 100, figs. 5(d)-5(f), led to a significant rise in the size of the convective cells, which was connected with the formation of the ascending air-flow near the bottom horizontal gas-wall interface. An increase in the length of the radiant heating source led to the deformation of the circulating flows. When $D = 0.75$, fig. 5(f), small-scale convective cells were formed near the top horizontal gas-wall interface, which was due to the shape of the convective torch. Further increase of the time to 300, fig. 5(g)-5(i) led to a slight modification of the streamlines.

Investigation of heat-retaining properties of enclosure structures

We calculated the heat accumulated by enclosures, tab. 2, in order to estimate the impact of the heat-retaining properties of the materials with different thermophysical characteristics on the energy losses to the walls.

It was established that the greater the heat conduction coefficient, the more thermal energy was accumulated by the finite thickness walls and, correspondingly, the less by air. As the result, the temperature and air velocity were decreased in the gas cavity. When heat conduc-

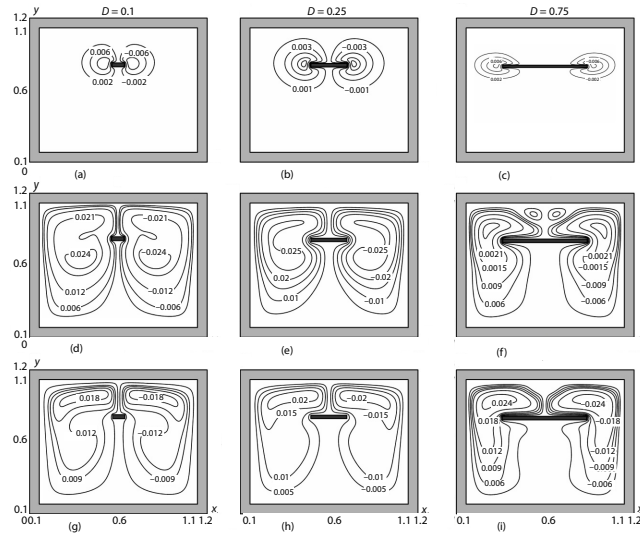


Figure 5. Streamlines for various transverse sizes of radiant heating source and $Ra = 10^6$; (a), (b), (c) $\tau = 10$, (d), (e), (f) $\tau = 100$, (g), (h), (i) $\tau = 300$

Table 2. Heat accumulated by bricks (Q_1), steel concrete (Q_2), and foam concrete (Q_3)

τ	Q_1 , [MJ]	Q_2 , [MJ]	Q_3 , [MJ]
	$\lambda = 0.7$ [WK ⁻¹ m ⁻¹]	$\lambda = 1.7$ [WK ⁻¹ m ⁻¹]	$\lambda = 0.1$ [WK ⁻¹ m ⁻¹]
500	1.07	1.32	0.48
1500	1.17	1.4	0.61
3000	1.29	1.51	0.76

gas-wall interface. With $Ra = 10^6$, natural convective effects dominated over conductive. The thickness of the convective torch decreased. This was due to an increase in the buoyancy force. An increase in the emitter length was visualized in the temperature rising in the area of $0.1 < X < 1.1$, $0.8 < Y < 1.1$, fig. 6. However, isotherms modified slightly. The conjugate formulation allows taking into account not only the heat-retaining properties of the finite thickness walls, but also the relevant changes of the temperature fields in dependence to the values of the Rayleigh numbers [17].

Figure 7 presents temperature distributions for various Rayleigh numbers in the cross-section of $Y = 0.95$.

With reference to fig. 7 it was established that an increase in the buoyancy force led to a rise in the temperature in the characteristic cross-section along the Y -axis, which was connected with the intensification of the heat transfer process. As the result, air velocity coming to the top horizontal gas-wall interface was increased. In this case, the point of maximum temperature was located in the section of $X = 0.6$, which could be explained by the form of the convective torch, fig. 6(c)-6(i) under the appropriate Rayleigh numbers.

tion coefficient was increased 17 times, tab. 2, finite thickness wall accumulated almost 90% more energy.

Investigation of the Rayleigh number impact on the heat transfer rate

Figure 6 presents transition dynamics from conductive to convective heat transfer mode in the physical conditions under consideration.

It was clearly seen that an increase in the Rayleigh number led to a significant isotherms modification. When $Ra = 10^4$, figs. 6(a)-6(c), conduction was pre-dominant heat transfer mechanism, which was proved by the shape of the isotherms in the gas cavity. The area of high temperature air was formed near the infrared emitter. When $Ra = 10^5$, the convective torch was formed at the top horizontal surface of the radiant heating source. The temperature in the area of $0.1 < X < 1.1$, $0.7 < Y < 0.75$, figs. 6(d)-6(f), decreased, which was obviously due to the moving of heated air to the top horizontal

Conclusions

According to the results of mathematical modelling of the conjugate natural convection in a closed rectangular cavity under conditions of the intense radiant heating, the main findings are as follows.

- The conjugate heat transfer process under study had a significant unsteady nature, which was proved by obtained fields of temperature and stream function in a dimensionless time range of $10 < \tau < 1200$.
- An increase in the emitter length in a range of led to a significant rise in the average temperature in the solution domain. However, isolines of temperature and stream function modified slightly.
- Variation of the heat conduction coefficient of the finite thickness walls in a range of $0.1 \leq \lambda \leq 1.7$ led to a rise in the energy accumulation by about 90%.
- Conduction was pre-dominant heat transfer mechanism at the low values of the Rayleigh number ($Ra \leq 103$). When $Ra = 105$, transition from conductive to natural convective heat transfer mechanism occurred in the conditions under consideration. Further increase in Rayleigh number ($Ra = 106$) led to convective plume formation near the bottom horizontal gas – wall interface and radiant energy source.

Further studies can include the analysis of the turbulent regimes of natural convection, applying net flux method when modelling radiative heat exchange and 3-D formulation of boundary value problem.

Acknowledgment

The reported research was supported by Russian Federation President Grant for state support of the Russian Federation leading scientific schools SS-7538.2016.8. In addition, the authors would also like to thank the reviewers for their constructive comments and suggestions.

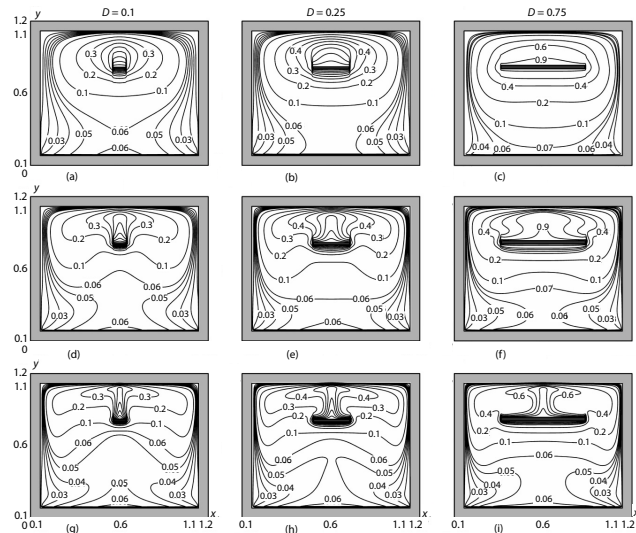


Figure 6. Isotherms for various transverse sizes of radiant heating source and $\tau = 300$; (a), (b), (c) $Ra = 104$, (d), (e), (f) $Ra = 105$, (g), (f), (i) $Ra = 106$

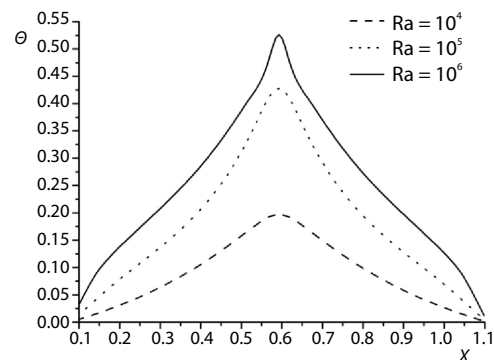


Figure 7. Temperature distributions at $\tau = 300$ in the section of $Y = 0.95$

Nomenclature

F_o	– Fourier number ($= at_0/L^2$), [–]
g	– gravitational acceleration, [ms^{-2}]
Ki	– Kirpichev number [$= qL\lambda^{-1}(T_h - T_0)^{-1}$], [–]
L	– transverse size of gas cavity, [m]
Nu_{av}	– average Nusselt number, [–]
Pr	– Prandtl number, [–]
Ra	– Rayleigh number [$= g\beta(T_h - T_0)L^3\nu^{-1}\alpha^{-1}$], [–]
T_0	– initial temperature, [K]
T	– temperature, [K]
T_h	– temperature on the surface of emitter, [K]
t_0	– time scale, [s]
t	– time, [s]
u, v	– velocities on the x - and y -axes, respectively, [ms^{-1}]
U, V	– dimensionless analogues of u, v , [–]
V_{nc}	– velocity scale, [ms^{-1}]
x, y	– cartesian co-ordinates, [m]
X, Y	– dimensionless analogues of x, y , [–]

Greek symbols

α	– thermal diffusivity, [m^2s^{-1}]
β	– coefficient of thermal expansion, [K^{-1}]
Θ	– dimensionless temperature, [–]
λ	– heat conduction coefficient, [$\text{WK}^{-1}\text{m}^{-1}$]
ν	– kinematic viscosity, [m^2s^{-1}]
τ	– dimensionless time, [–]
Ψ	– dimensionless stream function analogue, [–]
ψ	– stream function, [m^2s^{-1}]
ψ_0	– scale of stream function, [m^2s^{-1}]
Ω	– dimensionless analogue of vortex velocity vector, [–]
ω	– vortex velocity vector, [s^{-1}]
ω_0	– scale of vortex velocity vector, [s^{-1}]

Subscripts

1	– gas
2	– enclosures
3	– radiant energy source

References

- [1] Sadin, R., et al., The Effect of Temperature and Slice Thickness on Drying Kinetics Tomato in the Infrared Dryer, *Heat and Mass Transfer*, 50 (2014), 4, pp. 501-507
- [2] Zhu, K., et al., Experimental Study on the Optimization of Heat and Mass Transfer of Industrial Drying of the TiO_2 Bulb by Infrared Radiation, *Journal of Thermal Science*, 5 (1996), 4, pp. 278-284
- [3] El-Mesery, H. S., Mwithiga, G., Performance of a Convective, Infrared and Combined Infrared-Convective Heated Conveyor-Belt, D., *Journal of Food Science and Technology*, 52 (2015), 5, pp. 2721-2730
- [4] Sudarushkin, Y. K., et al., Convective-Infrared Drying of a Polyamide-Based Composite in a Fluidized Bed, *Russian Journal of Applied Chemistry*, 78 (2005), 12, pp. 1977-1980
- [5] Allanic, N., et al., Convective and Radiant Drying of a Polymer Aqueous Solution, *Heat and Mass Transfer*, 43 (2007), 10, pp. 1087-1095
- [6] Franz, F. P., et al., Investigations on the Heating and Drying of Wood with Infrared Radiation, *Wood Science and Technology*, 1 (1967), 2, pp. 149-160
- [7] Seyam, S., et al., Experimental and Numerical Investigation of the Radiant Panel Heating System Using Scale Room Model, *Energy and Buildings*, 82 (2014), Oct., pp. 130-141
- [8] Aich, W., et al., Numerical Analysis of Natural Convection in a Prismatic Enclosure, *Thermal Science*, 15 (2011), 2, pp. 437-446
- [9] Cho, C.-C., et al., Numerical Investigation into Natural Convection Heat Transfer Enhancement of Copper-Water Nanofluid in a Wavy Wall Enclosure, *Thermal Science*, 16 (2012), 5, pp. 1309-1316
- [10] Jani, S., et al., Numerical Investigation of Natural Convection Heat Transfer in a Symmetrically Cooled Square Cavity with a Thin Fin on its Bottom Wall, *Thermal Science*, 18 (2014), 4, pp. 1119-1132
- [11] Ghachem, K., et al., Numerical Study of Heat and Mass Transfer Optimization in a 3-D Inclined Solar Distiller, *Thermal Science*, 21 (2017), 6, pp. 2469-2480
- [12] Ahmanache, A., Zeraibi, N., Numerical Study of Natural Melt Convection in Cylindrical Cavity with Hot Walls and Cold Bottom Sink, *Thermal Science*, 17 (2013), 3, pp. 853-864
- [13] Saravanan, S., Sivaraj, C., Combined Natural Convection and Thermal Radiation in a Square Cavity with a Non-Uniformly Heated Plate, *Computers & Fluids*, 117 (2015), Aug., pp. 125-138
- [14] Montiel-Gonzales, M., et al., Theoretical and Experimental Study of Natural Convection with Surface Thermal Radiation in a Side Open Cavity, *Applied Thermal Engineering*, 75 (2015), Jan., pp. 1176-1186
- [15] Zhao F.-Y., et al., Conjugate Natural Convection in Enclosures with External and Integral Heat Source, *International Journal of Engineering Science*, 44 (2006), 3-4, pp. 148-165
- [16] Saaid, N. H., Conjugate Natural Convection in a Vertical Porous Layer Sandwiched by Finite Thickness Wall, *International Communications in Heat and Mass Transfer*, 34 (2007), 2, pp. 210-216

- [17] Kuznetsov, G. V., *et al.*, Heat Transfer under Heating of a Local Region of a Large Production Area by Gas Infrared Radiators, *Journal of Engineering Physics and Thermophysics*, 86 (2013), 3, pp. 519-524
- [18] Kuznetsov G. V., Sheremet M. A., Conjugate Natural Convection in an Enclosure with Local Heat Sources, *Computational Thermal Sciences*, 1 (2009), 3, pp. 341-360
- [19] Hamimid, S., Guellal, M., Numerical Analysis of Combined Natural Convection – Internal Heat Generation Source – Surface Radiation, *Thermal Science*, 20 (2014), 6, pp. 1879-1889
- [20] Kolsi, L., *et al.*, Combined Radiation – Natural Convection in Three-Dimensional Vertical Cavities, *Thermal Science*, 15 (2011), Suppl. 2, pp. S327-S339
- [21] Montiel-Gonzales, M., *et al.*, Numerical Study of Heat Transfer by Natural Convection and Surface Thermal Radiation in an Open Cavity Receiver, *Solar Energy*, 86 (2012), 4, pp. 1118-1128
- [22] Nounanegue, H. F., *et al.*, Heat Transfer by Natural Convection, Conduction and Radiation in a Inclined Square Enclosure Bounded with a Solid Wall, *International journal of Thermal Science*, 48 (2009), 5, pp. 871-880
- [23] Saravanan, S., Sivaraj, C., Coupled Thermal Radiation and Natural Convection Heat Transfer in a Cavity with a Heated Plate Inside, *International Journal of Heat and Fluid Flow*, 40 (2013), Apr., pp. 54-64
- [24] Kuznetsov G. V., *et al.*, Heat Transfer under Heating of a Local Region of a Large Production Area by Gas Infrared Radiators, *Journal of Engineering Physics and Thermophysics*, 86 (2013), 3, pp. 519-524
- [25] Nee A. E., Nagornova, T. A., Numerical Investigation of Conjugate Heat Transfer in a Local Working Area in Conditions of its Radiant Heating, *IOP Conference Series: Materials Science and Engineering*, 66 (2014), 012041
- [26] Kuznetsov, G. V., *et al.*, Computational Modeling of Conjugate Heat Transfer in a Closed Rectangular Domain under the Conditions of Radiant Heat Supply to the Horizontal and Vertical Surfaces of Enclosure Structures, *Journal of Engineering Physics and Thermophysics*, 88 (2015), 1, pp. 168-177
- [27] Modest, M. F., *Radiative Heat Transfer*, Elsevier Science, New York, USA, 2003
- [28] Roache, P. J., *Computational Fluid Dynamics*, Hermosa Publishers, Albuquerque, N. Mex., USA, 1976
- [29] Samarskii, A. A., *The Theory of Difference Schemes* (in Russian), Nauka, Moscow, 1977
- [30] De Vahl Davis, G., Natural Convection of Air in a Square Cavity: A Benchmark Numerical Solution, *International Journal of Numerical Methods in Fluids*, 3 (1983), 3, pp. 249-264
- [31] Dixit H. N., Babu, V., Simulation of High Rayleigh Number Natural Convection in a Square Cavity Using the Lattice Boltzmann Method, *International Journal of Heat and Mass Transfer*, 49 (2006), 3-4, pp. 727-739
- [32] Markatos, N. C., Pericleous, K. A., Laminar and Turbulent Natural Convection in an Enclosed Cavity, *International Journal of Heat and Mass Transfer*, 27 (1984), 5, pp. 755-772